Identification of new members of Fertilisation Independent Seed Polycomb Group pathway involved in the control of seed development in *Arabidopsis thaliana*

Anne-Elisabeth Guitton[1], Damian R. Page[2], Pierre Chambrier[1], Claire Lionnet[1], Jean-Emmanuel Faure[1], Ueli Grossniklaus[2] and Frédéric Berger[1,*]

[1]EMBO YIP Team, Unité Mixte de Recherche 5667, IFR128 BioSciences Lyon-Gerland, Ecole Normale Supérieure de Lyon, 46 allée d'Italie, F-69364 Lyon cedex 07, France
[2]Institute of Plant Biology and Zürich-Basel Plant Science Center, University of Zürich, Zollikerstrasse 107, CH-8008 Zürich, Switzerland
*Author for correspondence (e-mail: frederic.berger@ens-lyon.fr)

Accepted 12 March 2004

Development 131, 2971-2981
Published by The Company of Biologists 2004
doi:10.1242/dev.01168

Summary

In higher plants, double fertilisation initiates seed development. One sperm cell fuses with the egg cell and gives rise to the embryo, the second sperm cell fuses with the central cell and gives rise to the endosperm. The endosperm develops as a syncytium with the gradual organisation of domains along an anteroposterior axis defined by the position of the embryo at the anterior pole and by the attachment to the placenta at the posterior pole. We report that ontogenesis of the posterior pole in *Arabidopsis thaliana* involves oriented migration of nuclei in the syncytium. We show that this migration is impaired in mutants of the three founding members of the *FERTILIZATION INDEPENDENT SEED* (*FIS*) class, *MEDEA* (*MEA*), *FIS2* and *FERTILIZATION INDEPENDENT ENDOSPERM* (*FIE*). A screen based on a green fluorescent protein (GFP) reporter line allowed us to identify two new loci in the *FIS* pathway, *medicis* and *borgia*. We have cloned the *MEDICIS* gene and show that it encodes the *Arabidopsis* homologue of the yeast WD40 domain protein MULTICOPY SUPRESSOR OF IRA (MSI1). The mutations at the new *fis* loci cause the same cellular defects in endosperm development as other *fis* mutations, including parthenogenetic development, absence of cellularisation, ectopic development of posterior structures and overexpression of the GFP marker.

Movies and supplemental data available online

Key words: *Arabidopsis thaliana*, Endosperm, Seed, FIS, Polycomb, MSI1

Introduction

In the flowering plant *Arabidopsis thaliana*, double fertilisation initiates seed development (reviewed by Raghavan, 2003). One sperm cell fertilises the egg cell and initiates embryogenesis and a second sperm cell fertilises the central cell that develops into the endosperm. Endosperm development initiates as a syncytium. The endosperm is part of the seed and is thought to play an essential role in the control of maternal nutrient fluxes to the embryo. After four cycles of synchronous syncytial divisions, three mitotic domains are established along the anteroposterior axis of the endosperm and define the anterior micropylar, the peripheral and the posterior chalazal domains (Boisnard-Lorig et al., 2001). At the eighth mitotic cycle, cellularisation of the syncytial endosperm is initiated in the anterior domain around the embryo, prior to cellularisation of the peripheral domain (Sørensen et al., 2002). In contrast, the posterior endosperm does not cellularise and consists of multinucleate masses of cytoplasm, defined as the cyst at the most posterior location, and as nodules when located at the anterior part of the cyst (Scott et al., 1998). The organisation of a specialised posterior pole has been widely conserved through evolution (Floyd and Friedman, 2000). In *Arabidopsis*, mitotic division has not been observed in the posterior domain and the origin of the several nuclei present in this domain has remained unclear.

In *Arabidopsis*, the genes *MEDEA* (*MEA*) and *FERTILIZATION INDEPENDENT SEED 2* (*FIS2*) encode the Polycomb group (PcG) protein homologues of Enhancer of zeste (E(Z)) and Suppressor of zeste 12 (SU(Z)12) in *Drosophila*, respectively (Grossniklaus et al., 1998; Luo et al., 1999). MEA interacts in a PcG complex with the *Arabidopsis* homologue of Extra Sex Combs (ESC), FERTILIZATION INDEPENDENT ENDOSPERM (FIE) (Ohad et al., 1999; Luo et al., 2000; Spillane et al., 2000; Yadegari et al., 2000) and FIS2 is likely to be a third member of this PcG complex (Berger and Gaudin, 2003; Köhler et al., 2003a; Reyes and Grossniklaus, 2003). The *fis* mutants were originally isolated for the capacity to initiate seed development in absence of fertilisation (Peacock et al., 1995; Ohad et al., 1996; Chaudhury et al., 1997). Autonomous seeds do not contain an embryo but only endosperm.

Another original feature shared by *fis* mutants is a gametophytic maternal effect on seed abortion. The *FIS* class gene *MEA* was originally identified in a screen for female

gametophytic mutants affecting embryo sac development and function or displaying maternal effects (Grossniklaus et al., 1998). Seeds derived from female gametophytes carrying a mutation in one of the *FIS* genes abort irrespective of whether the paternal allele is mutant or wild type (WT). Among other phenotypes, the *fis* class mutants for *FIE*, *MEA* and *FIS2* are all characterised by an abnormal development of the endosperm posterior pole with a cyst and nodules larger than in the WT and the ectopic location of nodules in the peripheral endosperm (Sørensen et al., 2001). The endosperm of *fis* mutants shares other common features such as the absence of cellularisation and overproliferation at late stages (Kiyosue et al., 1999; Vinkenoog et al., 2000; Sørensen et al., 2001).

We have previously isolated the enhancer trap green fluorescent protein (GFP) marker line KS117 that displays uniform GFP expression in the endosperm until the embryo dermatogen stage and later becomes confined to the posterior pole (Haseloff, 1999) (http://www.plantsci.cam.ac.uk/Haseloff). In contrast to the WT, KS117 GFP expression in a *fis* mutant background is uniform throughout endosperm development and dramatically over-expressed as early as the embryo octant stage (Sørensen et al., 2001).

In this study, we took advantage of KS117 GFP reporter gene expression to compare the dynamics of endosperm posterior pole formation in the WT and *fis* mutants. We screened for altered KS117 GFP expression to identify mutants that showed defects in endosperm patterning pertaining to the posterior pole. We isolated two new members of the *fis* class, *medicis* and *borgia*. *MEDICIS* encodes the WD40 domain protein MSI1 that has recently been demonstrated to directly interact with the FIS class protein FIE in the MEA/FIE PcG complex (Köhler et al., 2003a). Although *medicis* and *borgia* display autonomous endosperm development as do other *fis* mutants, they show distinctive genetic and phenotypic features.

Materials and methods

Plant material and growth conditions

The KS117 enhancer-trap line was generated in J. Haseloff's lab (www.plantsci.cam.ac.uk/Haseloff/home.html) and was described previously (Sørensen et al., 2001). *fis1/mea*, *fis2-3*, *fis3/fie* lines were provided by A. Chaudhury (Chaudhury et al., 1997). *MET1* a/s line was provided by J. Finnegan (Finnegan et al., 1996). Plants were grown at 20°C in a growth chamber with a 12-hour day/12-hour night cycle until they formed rosettes. Flowering was then induced at 22°C with a 16-hour day/8-hour night cycle in a greenhouse. Autonomous seed development was obtained after emasculation of mature flower buds under greenhouse conditions. Pistils were harvested 7 days after emasculation.

Microscopy and image processing

Developing seeds were isolated from individual siliques at different stages of development. Each population of seed was mounted in Hoyer's medium (Boisnard-Lorig et al., 2001) and fluorescence associated to the KS117 marker was readily observed with a Leica MZFLIII stereomicroscope coupled to a DC300F digital camera (Leica Microsystems, Heerburg, Germany). Images were processed with the FW4000 software (Leica). Endosperm size was measured using Image J (software available at rsb.info.nih.gov/ij/) in WT and mutant populations of seeds. After clearing in Hoyer's medium, the phenotype was determined microscopically using differential interference contrast **(**DIC) optics (Optiphot, Nikon, Tokyo, Japan) coupled with an AxioCam MRc digital camera (Carl Zeiss, Jena, Germany) and linked for each seed to the associated genotype determined by the expression of KS117 GFP. Images were processed with Axiovision software (Zeiss).

For confocal microscopy, seeds were stained with Feulgen as described previously (Garcia et al., 2003) and examined with a Zeiss LSM 510 microscope with a ×63 Plan-Apochromat oil immersion objective (n. a. 1.4). Serial optical sections of 0.4 μm to 0.6 μm depth were recorded. Nucleoli were manually segmented on each section with Image J, recorded as an individual stack of images which was eventually subtracted from the original stack. Resulting stacks were imported as separate channels in the Imaris software (Bitplane AG, Zürich, Switzerland), pseudocoloured in white, red or yellow and visualised as a 3D volume. All figures were composed with Adobe Photoshop 5.5 (Adobe Systems, San Jose, USA).

Time-lapse imaging of NCDs migration

Seeds from plants homozygous for the marker KS22 (Boisnard-Lorig et al., 2001) were used for analysis of the WT and from plants heterozygous for *fis1/mea*, *fis2-3* and *fie-10* and homozygous for KS117 for analysis of KS117 reporter gene expression in *fis* mutant backgrounds. Freshly isolated siliques were prepared as described previously in order to be able to perform time-lapse analysis of NCDs migration (Boisnard-Lorig et al., 2001). Seeds oriented in such a way that the endosperm posterior pole was included in the confocal plane were selected for examination. Sections with 1024×1024 pixels were typically recorded every 10 minutes for at least 12 hours using a ×20 (n. a. 0.4) Ph2 Achroplan objective (Carl Zeiss, Jena, Germany) and a LSM510 Zeiss confocal laser scanning microscope. AVI films were mounted using the software Metamorph.

Genetic screen

4000 M_1 plants were grown from KS117/KS117 gamma-ray irradiated seeds (200 gray at a rate of 27 gray/minute) and the main stem cut to allow development of lateral sectors. One sector was chosen per plant and one silique was slit open and seeds examined at the green embryo stage. The presence of 10% semi-sterile mutation (absence of development of 50% of seeds), 8% embryo lethal mutation (collapsed seeds) and 1.1% albino mutations (seeds with a white embryo) was recorded. These percentages compared with those obtained in EMS screens (Jürgens et al., 1991) allowed us to estimate the expected allelic frequency of the screen to be one to two alleles per mutation. In parallel, we mounted a small population of seeds isolated from one or two siliques in mounting medium on a microscope slide. Mounting medium consisted of 0.3% plant agar (Duchefa, The Netherlands) in Murashige and Skoog culture medium (Sigma, Saint-Quentin Fallavier, France). Seeds were isolated at the embryonic heart stage when KS117 expression is confined to the posterior pole in the WT. We observed GFP fluorescence patterns of the KS117 marker using a Leica MZFLIII stereomicroscope equipped with a ×1.6 planApo objective (Leica, Jena, Germany) coupled to a DC300F digital camera (Leica Microsystems, Heerburg, Germany). Images were processed with the FW4000 software (Leica). Four backcrosses to WT KS117/KS117 were performed for each line.

Genetic mapping

F_2 mapping populations were generated by crossing each mutant line to WT Columbia. Putative alleles of *mea*, *fis2*, *fie* and *dme* were identified through a low recombination rate with the following markers, respectively: nT7i23 (for primer sequences, see the TAIR database (www.arabidopsis.org), fis2sslp (5′-AATTGAGCCCTTT-GACGTTTTGGTA-3′ and 5′-CCTGCATTGTTTGGGAGTGATA-GAA-3′), CER456484 [designed from Cereon database (www.arabidopsis.org/Cereon/index.html) (Jander et al., 2002)], 5′-AACCCTAAAGCTAGAGTTTATAGC-3′ and 5′-CCAAGCTCTAA-GCCAATCAGAGAAG-3′) and CER479331 (Cereon, 5′-GACGTC-GAGCGTAGATAGCACGC-3′ and 5′-CTGGTGGTCCTACGTTCC-GATTCAAG-3′). Allelism to *mea*, *fie* or *dme* was confirmed by direct

sequencing of the gene in the mutant line and comparison to the WT sequence. Allelism to *fis2* was confirmed by phenotypic complementation. The putative *fis2* alleles JF2034 and JF2206 were crossed as homozygotes with a line containing the 18H1 cosmid containing a wild-type copy of *FIS2* linked to kanamycin resistance (Kan^R) (Luo et al., 1999). F_1 plants were heterozygous for the mutation and hemizygous for 18H1. In F_1 plants, half the mutant ovules carry a WT copy of *FIS2* provided by 18H1 cosmid. Thus, if complementation takes place, only 25% of seeds are expected to display the mutant phenotype in contrast to a selfed heterozygote *fis2* mutant that produces 50% mutant seeds. Four independent Kan^R F_1 plants were analysed for each line and showed 25% mutant seeds instead of the 50% observed in heterozygous plants [JF2034×18H1 no. 1: 23.7% mutant seeds (s.d. 6.5); no. 2: 27.3% (4.5); no. 3: 25.2% (5.5); no. 4: 24.2% (4.6). JF2206×18H1 no. 1: 24.7% (4.3); no. 2: 21.7% (3.2); no. 3: 24.4% (5.5); no. 4: 22.5% (2.6)]. The locus associated with the *bga* mutation was located between TAIR markers PLS7 and nga1126. *MEDICIS* was shown to be located between MTI20.1/2 (Cereon, 5′-AACCGTTTTCCATATCTTATTCTC-3′ and 5′-TCAAATCATACAACTACGAAAGTC-3′) and K19M22.4/5 (Cereon, 5′-AGGTAATTGGGCCAGGAACTAAAT-3′ and 5′-CCAAACGGGAGTAAATCATCTGGTG-3′).

Results

Ontogeny of endosperm posterior pole involves oriented migrations of nuclei

Until the embryo dermatogen stage when the syncytial endosperm has undergone six mitotic divisions and contains approximately 50 nuclei, the posterior pole contains two or four nuclei that do not divide but become larger as a result of endoreduplication cycles (Boisnard-Lorig et al., 2001) (Fig. 1A). These large nuclei are at the centre of a mass of cytoplasm called the cyst and are surrounded by nuclei embedded in small masses of cytoplasm forming nuclear cytoplasmic domains (NCDs; *n*=22) (Brown et al., 1999). After the seventh cycle of syncytial nuclear division in the endosperm (early globular stage embryo) the cyst still contains two or four large nuclei and is surrounded by one or two NCDs containing two nuclei (Fig. 1B) (*n*=18). Until the next mitotic division that is followed by endosperm cellularisation (early heart stage embryo) four to seven NCDs with multiple nuclei are observed above the cyst. These structures, called nodules, contain up to ten nuclei (Fig. 1C) (*n*=68). In the cyst the large nuclei are surrounded by ten to 30 nuclei similar in size to the nuclei in NCDs (*n*=68). The origin of multinucleate nodules and the cyst is unknown. It could be explained either by divisions of nuclei within NCDs or by fusion of NCDs together or with the cyst. To distinguish between these two mechanisms, we performed time-lapse recording of endosperm posterior pole development (Fig. 2A; movie 1, http://dev.biologists.org/supplemental/). In the enhancer trap line KS22, NCDs are labelled with mGFP5 targeted to the endoplasmic reticulum and endosperm develops as in the WT (Boisnard-Lorig et al., 2001). Recordings were made after the seventh cycle of syncytial mitosis and show that this event is followed by migration of NCDs toward the cyst (Fig. 2A, 170 minutes) (*n*=10). We observed that a few NCDs fuse into the cyst (movie 1, http://dev.biologists.org/supplemental/). More frequently a NCD migrates toward another NCD located closer to the cyst and merges with it. The fusion of two NCDs constitutes a binucleate nodule (Fig. 2A, 370-430 minutes). Nodules incorporate other NCDs (Fig. 2A, 590-660 minutes) and eventually migrate and merge with the cyst (movie 1, http://dev.biologists.org/supplemental/). Migration of NCDs takes place within 30-60 minutes for relatively short distances (30-60 μm) along the anteroposterior axis toward the posterior pole (*n*=45). We conclude that the posterior pole undergoes a series of fusions of NCDs becoming nodules that eventually migrate and fuse into the cyst. These events affect only the population of NCDs at the posterior pole. This population increases as a result of

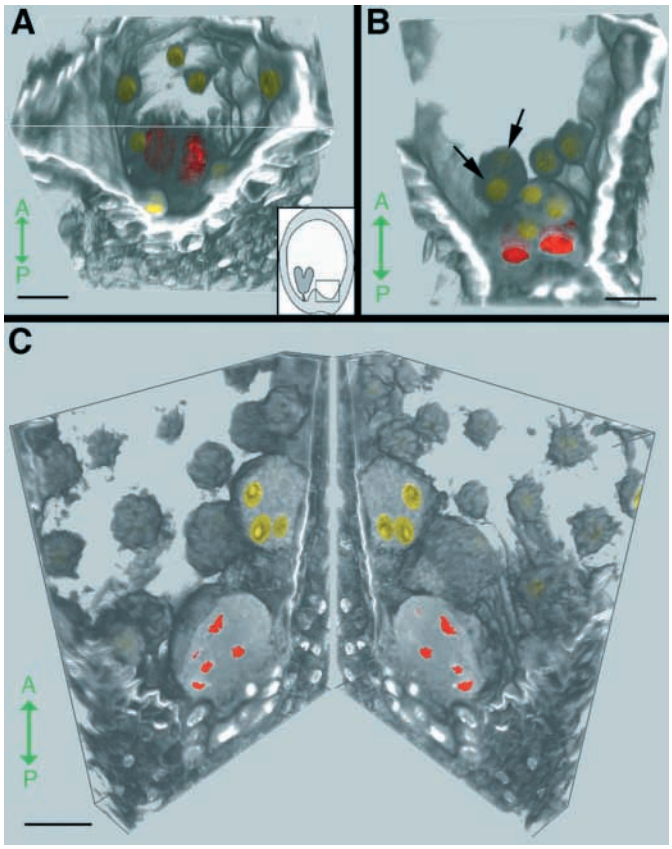

Fig. 1. Ontogeny of the endosperm posterior pole. 3D reconstruction of the endosperm posterior pole. Inset shows the location of the posterior pole in a schematic whole seed. Nuclei in the cyst have been labelled in red and other nuclei in yellow. The anteroposterior (AP) axis is indicated by the green double arrow. (A) Embryo dermatogen stage, endosperm stage VII with approx. 50 nuclei. Two large nuclei in the cyst have undergone two cycles of endoreduplication and are embedded in a pool of cytoplasm. Other nuclei in the peripheral domain are surrounded by a small mass of cytoplasm that constitutes a NCD. Scale bar: 25 μm. The 3D reconstruction was obtained from 85 optical sections of 0.4 μm thickness. (B) Early globular stage embryo, endosperm stage VIIIa with approx. 100 nuclei. Above the cyst that still contains only two large nuclei, are two masses of cytoplasm that each contain two nuclei (arrows). Other NCDs are still attached to the walls of the peripheral endosperm. Scale bar: 25 μm. The 3D reconstruction was obtained from 46 optical sections of 0.65 μm thickness. (C) Early heart stage embryo, endosperm stage IX with cellularisation initiated in the micropylar endosperm at the anterior pole (not visible). The 3D reconstruction is represented as an open book split in the middle, along a plane aligned with the anteroposterior axis. The cyst contains multiple nuclei of similar size to those in NCDs. Above the cyst, are observed seven nodules that contain from two up to ten nuclei. In more anterior domains, free NCDs line the wall of the peripheral endosperm. Scale bar: 50 μm. The 3D reconstruction was obtained from 96 optical sections of 0.4 μm thickness.

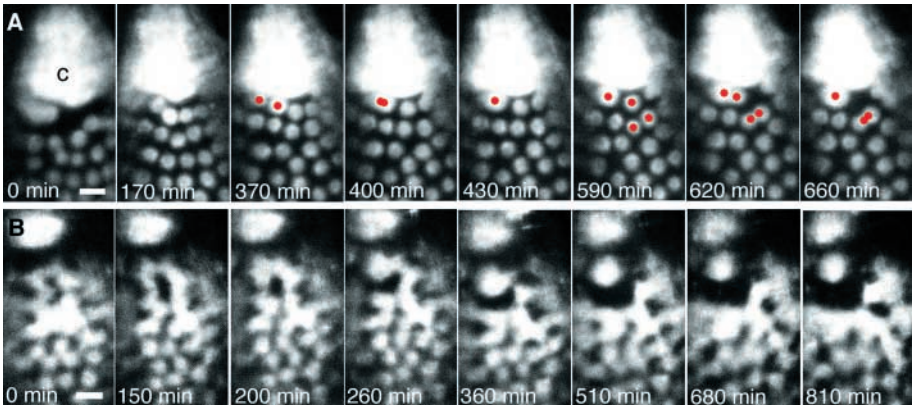

Fig. 2. Live imaging of migration and fusions of NCDs at the endosperm posterior pole. (A) Confocal sections selected from a time-lapse series of 67 images acquired every 10 minutes. The whole video can be seen at http://dev.biologists.org/supplemental/. The endosperm endoplasmic reticulum is labelled with mGFP5 expressed under the control of the specific enhancer KS22 (Boisnard-Lorig et al., 2001). Hence each NCD is labelled individually and the cyst (c) appears as a large fluorescent mass at the posterior pole. The seventh mitotic division has taken place 40 minutes before time 0 minute. After mitosis, NCDs migrate toward the cyst (170 minutes). Later, a NCD migrates towards a neighbouring NCDs closer to the posterior pole and eventually fuses with it (370-430 minutes). The resulting nodule attracts a third NCD while other NCDs migrate and fuse (590-660 minutes). (B) A time-lapse series similar to the one shown in A, selected from 82 images acquired every 10 minutes, showing the absence of oriented migration and non-specific fusions of NCDs in the mutant *fis2-3* background. The seed was selected as *fis2-3* at the mid-globular stage on the basis of its strong fluorescence, persistent in all domains of the endosperm, provided by the activity of the enhancer KS117 that drives expression of mGFP5 (Sørensen et al., 2001). A mitotic division has taken place 20 minutes before time 0 minute and no posterior migration of NCDs is observed in comparison to WT. No specific migration nor oriented fusion is observed later in development and unusually large nodules assemble as a result of 'passive' engulfing by growing cytoplasm (360-510 minutes). Gradually, the polarised anteroposterior arrangement of NCDs, nodules and cyst is lost (810 minutes). Scale bars: 20 μm (all sections).

syncytial mitotic divisions and includes 25-30 nuclei after the eighth mitotic division. This division is followed by endosperm cellularisation. The posterior pole does not become cellular and nuclei in NCDs still undergo two further cycles of syncytial divisions until the early embryo torpedo stage (not shown). We have never observed divisions in nuclei present in the cyst and in the nodules. The embryo torpedo stage is marked by a decline in the number of NCDs as they are progressively absorbed by nodules that later fuse with the cyst. Ultimately, the posterior pole consists only of the multinucleate cyst (Fig. 3A).

Ontogeny of the endosperm posterior pole is disrupted in *fis* mutants

Previously, we have shown that mutations in the *fis* genes *mea*, *fis2* or *fie*, cause ectopic KS117 GFP expression in the endosperm of the marker line, and ectopic development of nodules (Sørensen et al., 2001) (Fig. 3B). This observation led to the hypothesis that endosperm anteroposterior polarity is perturbed in *fis* mutants. In this study, we analysed the origin of the ectopic nodules in vivo. In *fis2*/*FIS2;* KS117/KS117 plants, strong and uniform GFP expression identifies *fis2* seeds at the early globular embryo stage (Fig. 2B; movie 2, http://dev.biologists.org/supplemental/). In contrast to the WT, NCDs dynamics is strongly reduced and only limited migration is observed after the seventh mitotic syncytial division (movie 2, http://dev.biologists.org/supplemental/) (n=8). In a few cases, NCD migrations take place at random (not shown). The cyst does not appear to incorporate nodules (Fig. 2B) or undergo massive fusion with very large nodules. Nodules appear to assemble rather as the result of the growth of the cytoplasm that gradually engulfs a larger population of nuclei (Fig. 2B, Fig. 3B). Similar defects in posterior endosperm development were observed in *mea* and in *fie* backgrounds (not shown). In conclusion, *fis* mutations disrupt the oriented migration of NCDs and prevent proper differentiation of the endosperm posterior pole.

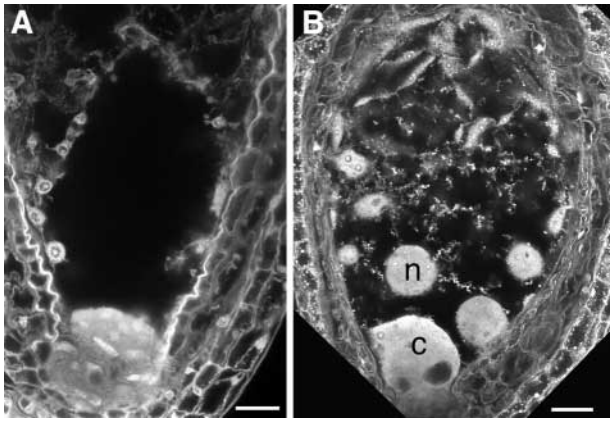

Fig. 3. Comparison of the organisation of the endosperm posterior pole in the WT and in *fis2-3*. (A) Confocal section of the endosperm posterior pole from the abaxial side of a WT seed at the torpedo stage. The endosperm is cellularised with the exception of the posterior pole that consists of the cyst containing nuclei with very dense chromatin. (B) In contrast to WT, *fis2* endosperm is not cellularised at the torpedo stage and its posterior pole consists of a large cyst (c) and multiple large multinucleate nodules (n). Nuclei in the cyst and in nodules show a chromatin organisation similar to nuclei in the peripheral endosperm. Scale bars: 20 μm.

Endosperm posterior pole formation is maternally controlled by a group of at least six loci associated with gametophytic mutations

To identify new members of the FIS pathway, we screened a population of developing M_2 seeds of 4000 M_1 plants for abnormal GFP expression from the posterior endosperm marker KS117. We identified ten putatively gametophytic mutants. As heterozygotes they produced 28-50% seeds that over-expressed KS117 GFP and did not restrict its expression

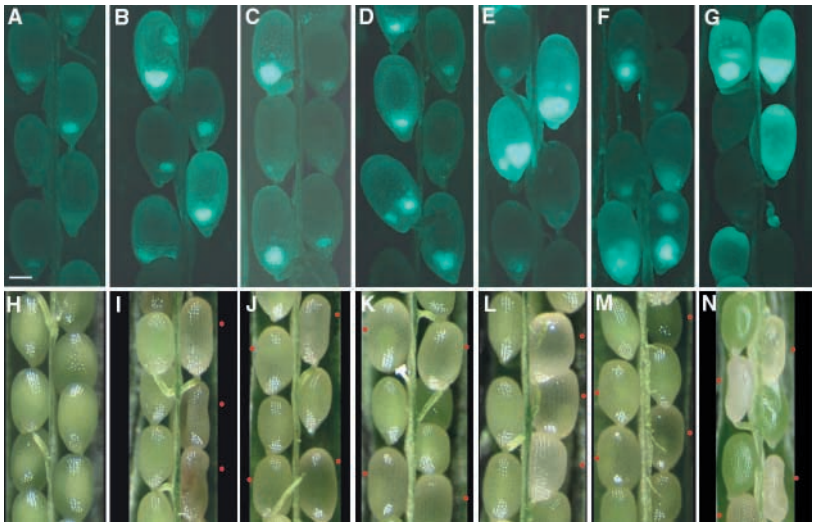

Fig. 4. Gametophytic maternal effect mutants with a *fis* phenotype. KS117 GFP is misexpressed. In mutant seeds, the level of GFP accumulation is much higher and the expression is not restricted to the posterior pole in mutant seeds. More than 25% of seeds abort. One line from each mutant group is presented here. (A-G) Seeds observed by epifluorescence stereomicroscopy. (H-N) Seeds observed by light microscopy. All aborting seeds are indicated by red dots. (A,H) WT KS117; (B,I) *dme-4/DME*; (C,J) *mea-6/MEA*; (D,K) *fis2-6/FIS2*; (E,L) *fie-11/FIE*; (F,M) *bga-1/BGA*; (G,N) *msi1-2/MSI1*. Scale bar: 200 μm (all images).

to the posterior pole (Fig. 4A-G). At the WT mature green embryo stage, mutant seeds are distinguished by a white translucent colour with a small green embryo (Fig. 4H-N). Eventually seed integuments collapse and shrivel around the embryos that arrest development at various stages after the heart stage. With the exception of JF0122, JF1762 and JF2973, plants homozygous for the mutation could be recovered from all other lines, showing that most of these mutations were not fully penetrant for seed lethality.

Production of more than 25% abnormal seeds by heterozygous plants suggested that we had isolated mutations with a gametophytic maternal control. To test this hypothesis, we reciprocally crossed each heterozygous mutant to WT. The seed-defective phenotype was only observed in the F_1 when the female was the mutant (Table 1). Together, these results suggest that in these ten mutants the phenotype was under gametophytic maternal control. A rate of 50% abortion was not reached in all mutants, showing differences in penetrance.

We first determined whether these ten mutants were new alleles of known *fis* class genes or were new loci. Allelism to known *fis* mutants was shown by genetic mapping (Table 1) and was then confirmed by complementation by a WT copy of the gene or by sequencing (Fig. S1, http://dev.biologists.org/supplemental/).

During the course of this work the mutant *demeter* (*dme*) was isolated and reported to be defective in transcriptional activation of *MEA* (Choi et al., 2002). *DME* is located on chromosome 5, close to the position we determined for JF1348, suggesting that JF1348 was allelic to *dme*. We sequenced *DME* in this mutant and could confirm the allelism (Fig. S1, http://dev.biologists.org/supplemental/).

For two lines that could be mapped to chromosome 2 and 5, respectively, JF1728 and JF2973, no tight linkage to any of the known *FIS* genes was detected, suggesting that these two mutants affected unknown genes. We named these two mutants *borgia* and *medicis*, respectively, as a reference to the Italian families of the Renaissance period who were particularly remarkable for a tradition of infanticide as was Medea in antique Greece. The *borgia* mutation is located in proximity of *FIS2* on chromosome 2 but *bga* location could be narrowed down to a region that does not contain *FIS2*, confirming that

Table 1. Ten gametophytic maternal effect mutants were isolated from a KS117-based screen.

	Reciprocal crosses: % mutant phenotypes*		Genetic mapping
Line no.	Mutant female × WT male (*n*)	WT female × mutant male (*n*)	Closest marker(s)†
JF1348 (*dme-4*)	43.8±5.3 (164)	0 (254)	CER479331 (0/138)
JF0531 (*mea-5*)	45.6±7.2 (274)	0 (263)	nT7i23 (0/44)
JF1760 (*mea-6*)	34.4±9.0 (103)	0 (218)	nT7i23 (0/66)
JF3206 (*mea-7*)	43.5±10.9 (123)	0 (110)	nT7i23 (0/66)
JF2034 (*fis2-6*)	47.7±2.7 (122)	0 (115)	Fis2sslp (0/68)
JF2206 (*fis2-7*)	39.0±7.3 (168)	0 (187)	Fis2sslp (0/70)
JF0122 (*fie-10*)	55.4±5.8 (74)	0 (148)	CER456484 (0/88)
JF1762 (*fie-11*)	47.1±15.8 (153)	0 (153)	CER456484 (0/88)
JF1728 (*bga-1*)	28.2±13.0 (301)	0 (238)	between PLS7 (7/142) and nga1126 (6/142)
JF2973 (*medicis, msi1-2*)	52.1±10.0 (691)	0 (295)	between MTI20.1/2 (2/736) and MZN1.1/2 (2/736)

n, Number of seeds.
*Values are means±s.d.
†Number of recombinant chromosomes/total chromosome number.
For each mutant, genetic data (reciprocal crosses between a heterozygote and a WT plant) show that the mutant phenotype is under gametophytic maternal control: a mutant maternal allele is sufficient to cause seed abortion, even when using wild-type pollen, whereas mutant pollen does not lead to abortion in any seed. Genetic mapping allowed us to determine which loci are affected in these lines. Tight linkage was found for one line with marker CER479331, for three lines with marker nT7i23, for two lines with marker fis2sslp, and for 2 lines with marker CER456484, suggesting that out of the 10 lines, 8 were allelic to one of the known *fis* mutants and two mutants had identified new loci, *borgia* (*bga*) and *medicis*, with a *fis*-like KS117 GFP expression phenotype.

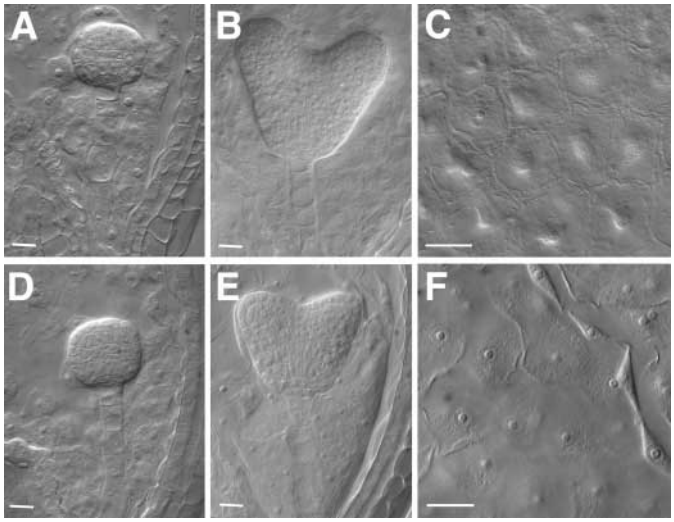

Fig. 5. Microscopic analysis of phenotypes in *bga/BGA* seeds. (A,B) WT embryos at mid globular and mid heart stage, respectively. (C) Cellularised endosperm in a WT seed at mid heart stage. (D,E) *bga/BGA* embryos in the same siliques as those in A and B, respectively. (F) Endosperm is not cellularised in a *bga/BGA* seed at the same stage as in C. Scale bars: 30 μm.

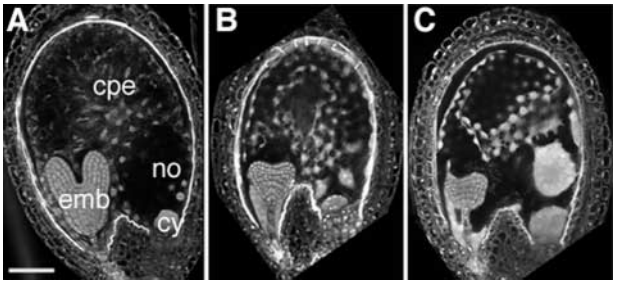

Fig. 6. Confocal sections of *bga-1* and *msi1-2* mutant seeds. (A) In WT seeds at early torpedo stage (emb), peripheral endosperm is cellularised (cpe). The cyst (cy) and small nodules (no) are visible at the posterior pole. (B) In siliques at the same stage, *bga* seeds show a delay in embryo development, although morphology is normal. Peripheral endosperm is not cellularised and the posterior pole overproliferates. (C) *msi1-2* seeds have arrested embryos. Peripheral endosperm is not cellularised and the posterior pole strongly overproliferates. Scale bar: 100 μm (A-C).

we had identified a new *fis* class locus on chromosome 2. We attribute the gene symbol *BGA* to this locus. Map-based cloning of *medicis* narrowed down the location of the mutation to a 280 kb interval that included the BACs MTI20, K21L19, MCK7 and MQJ2 on chromosome 5. This portion of the *Arabidopsis* genome contains the *MSI1* gene which was a candidate for the mutation. An orthologue of MSI1 in *Drosophila*, p55, is part of the PcG complex formed by genes homologous to the *FIS* genes *MEA*, *FIS2* and *FIE* (Tie et al., 2001). In the course of this work, we learned that a T-DNA insertion in *MSI1* was associated with a loss-of-function that caused a phenotype similar to the *fis* phenotype (Köhler et al., 2003a). Thus, we sequenced *MSI1* in *medicis* and identified a mutation leading to the production of a very short truncated protein (Fig. S1, http://dev.biologists.org/supplemental/). We hereafter refer to the *medicis* mutation as *msi1-2*.

In summary, the ten gametophytic mutants recovered from our screen identified three new *mea* alleles (hereafter referred to as *mea-5* to *mea-7*), two new *fis2* alleles (hereafter referred to as *fis2-6* and *fis2-7*), two new *fie* alleles (hereafter referred to as *fie-10* and *fie-11)*, and one allele each of *dme* (hereafter referred to as *dme-4*) and *msi1* (hereafter referred to as *msi1-2*). Importantly, our screen reveals the mutation *bga-1* in a new *fis* class locus on chromosome 2.

Effects of *bga* on seed development

Taking advantage of the differential KS117 GFP expression pattern between WT and *bga* seeds, we established a precise description of mutant seeds development. Mutant *bga* embryo development is similar to the WT until early heart stage (Fig. 5A,D). From the WT mid heart stage, mutant embryo development slows down (Fig. 5B,E) and eventually arrests between the late heart and the late torpedo stages when the WT embryos reach the mature green stage. Overall WT and mutant development of endosperm are similar until the endosperm contains 200 nuclei. At this stage, the WT endosperm cellularises, whereas the *bga* endosperm does not (n=114, Fig. 5C,F). Furthermore, an overgrowth of nodules and cyst is visible from this stage in the mutant endosperm and is amplified later in development (Fig. 6A,B). Seed size measurements show that *bga* and WT endosperms are similar in size, as it is the case for *fie-11* at this point of seed development (Table 2). Cellularisation is followed in the WT by one cycle of pseudo-synchronous cell division leading to an endosperm containing 400 nuclei. Only half of the mutant *bga* syncytial endosperms undergo this division (n=39), and endosperm nuclear proliferation is arrested in *bga* seeds after this stage.

Unlike other *fis* mutants, the *bga* phenotype affects only 28% seeds in siliques of *bga*/*BGA* plants fertilised by WT pollen (Table 1). No mutant phenotype was observed in seeds produced by reciprocal crosses, showing that *bga* mutation has a strict gametophytic maternal effect. Plants homozygous for *bga* are produced from seeds selected for a shrunken morphology. Transmission data confirm a high viability of the mutant embryos. When a *bga/BGA* plant is pollinated by *BGA/BGA* pollen, 21.5% (n=135 F_1 plants) *bga/BGA* plants are found in the F_1 progeny. In the reciprocal cross, fertilisation of a *BGA/BGA* plant by *bga/BGA* pollen gives rise to 45.5% (n=132) *bga/BGA* F_1 plants. Thus, the *bga* mutation is fully transmitted by male gametes, whereas transmission via the female gametes is reduced by half.

In conclusion, the *bga* mutation has a gametophytic maternal effect on embryo and endosperm development. The embryo is first delayed from the early heart stage and then arrested at late stages. Ectopic nodule formation occurs in *bga* endosperm as in other *fis* mutants, but in contrast to what was described previously for *mea* and for *fie* (Kiyosue et al., 1999; Vinkenoog et al., 2000), no overproliferation of endosperm nuclei was observed in *bga*.

msi1 has both sporophytic and gametophytic effects on seed development

When *msi1*/*MSI1* pistils are pollinated by WT plants, siliques contain 52% seeds showing a *fis* phenotype, while reciprocal

Table 2. Seed size and number of endosperm nuclei in *fie*, *bga* and *msi1* mutant seeds, at a stage corresponding to wild-type torpedo stage

Seed genotype	Seed length (μm) (s.d.)	Student's *t*-test	Seed width (μm) (s.d.)	Student's *t*-test	No. endosperm nuclei per seed
WT	283 (33) *n*=104		249 (33) *n*=104		400 (Scott et al., 1998)
fie-11/FIE	274 (37) *n*=47	*t*=1.49	246 (36) *n*=47	*t*=0.50	> 400 (Kiyosue et al., 1999; Vinkenoog et al., 2000)
bga-1/BGA	282 (62) *n*=21	*t*=0.11	241 (48) *n*=21	*t*=0.93	200 (79%) 400 (21%) *n*=86
msi1-2/MSI1	254 (33) *n*=69	*t*=5.66	223 (32) *n*=69	*t*=5.14	200 (49%) 400 (51%) *n*=39

Mean length and width of WT and mutant seeds are given in μm. A Student's *t*-test was carried out on the mean length or width in comparison to WT for each mutant. *t* values should be compared to the theoretical value of 1.96 (α=0.05). The number of nuclei contained in endosperm was determined after clearing of seeds at the same stage.

crosses produce only seeds with a WT phenotype (Table 1). These results show that the *msi1 fis*-like phenotype is under gametophytic maternal control. We were not able to obtain plants homozygous for *msi1* as a result of embryo lethality. Furthermore, transmission of the *msi1* allele via the female gametes is null (*n*=232 F_1 plants). Paternal transmission is also reduced in the *msi1* mutant, as only 36.2% F_1 plants (*n*=232) from pollination of WT pistil by *msi1/MSI1* bear the mutant allele. Mature pollen grains from *msi1/MSI1* plants contain two gametes and present a normal morphology (not shown) and the origin of reduced paternal transmission remains unknown.

When *msi1*/*MSI1* plants are self-pollinated only 30% of the seeds have a *fis* phenotype and 22% of the seeds display a distinct phenotype with severe embryo abnormalities. The distribution of the *fis* and abnormal embryo phenotypes in self-pollinated plants is 2 WT:1 *fis*-like:1 abnormal embryo (*n*=157, χ^2=2.22 $<\chi^2_{0.05[2]}$=5.991), suggesting that the abnormal embryo phenotype is under sporophytic recessive control.

KS117 GFP overexpression in mutant seeds allowed us to examine endosperm and embryo development in *msi1/MSI1* self-pollinated plants. The sporophytic recessive phenotype in embryos is distinguished as early as the WT octant stage. Improper cell division patterns are observed in the embryo proper and in the suspensor (Fig. 7A,G), leading to the development of a highly abnormal embryo (Fig. 7B,H). Endosperm that surrounds the arrested embryo does not differentiate a posterior chalazal pole nor cellularise, and nucleoli are variable in size (Fig. 7C,I). In the WT, syncytial endosperm development consists of synchronous nuclear divisions. In the mutant endosperm, we observed a delay of one cycle of division at each developmental stage, in comparison to WT seeds.

The phenotype associated with the gametophytic maternal effect is distinct from the sporophytic recessive effect. During the first steps of development, the pattern and timing of division of the mutant embryos are similar to those of the WT (*n*=196, Fig. 7A,D). When WT embryos reach the mid heart stage, mutant embryos are arrested at the early heart stage (*n*=103, Fig. 7B,E). Later in development, 7% mutant embryos (*n*=57) develop abnormally with extra layers of cells resulting from additional periclinal divisions (not shown), as described previously in *msi1-1* allele (Köhler et al., 2003a). In the

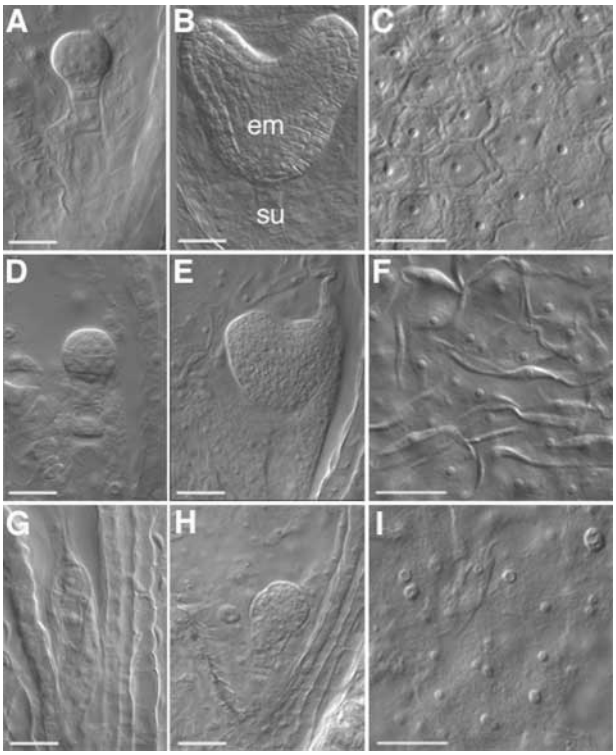

Fig. 7. Microscopic analysis of *msi1-2/MSI1* and *msi1-2/msi1-2* seeds. (A,B) WT embryo at dermatogen and mid heart stage, respectively. em: embryo proper, su: suspensor. (C) Cellularised endosperm in a WT seed at the same stage as in B. (D,E) *msi1-2/MSI1* embryos in same siliques as A and B, respectively. (F) Endosperm is not cellularised in a *msi1-2/MSI1* seed at the same stage as in C. (G,H) *msi1-2/msi1-2* embryos in same siliques as A and B, respectively. (I) Endosperm is not cellularised in a *msi1-2/msi1-2* seed at the same stage as in C. Nucleoli are variable in size. Scale bars: 50 μm.

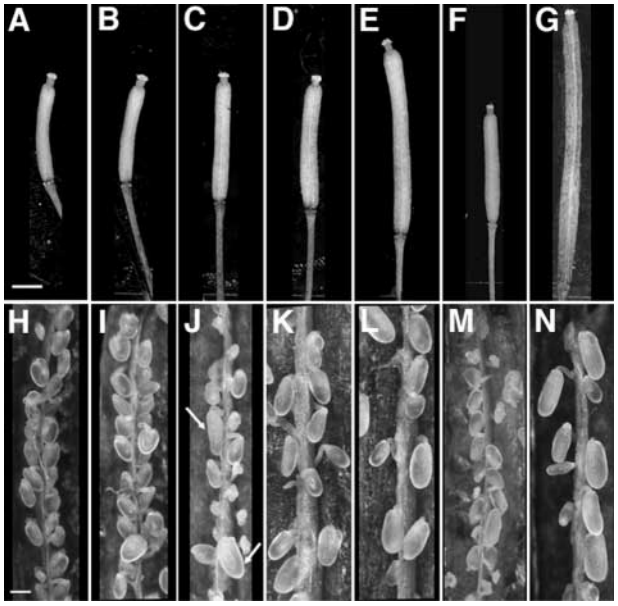

Fig. 8. Autonomous seed development in gametophytic maternal effect mutants. Mature flower buds were emasculated. (A-G) After 7 days, pistil elongation was scored. Scale bar: 1 mm. (H-N) Pistils were then slit open in order to observe seeds (arrows) and undeveloped ovules. Scale bar: 200 μm. (A,H) WT KS117; (B,I) *dme-4/DME*; (C,J) *mea-6/MEA*; (D,K) *fis2-6/FIS2*; (E,L) *fie-11/FIE*; (F,M) *bga-1/BGA*; (G,N) *msi1-2/MSI1*.

endosperm, the overall pattern and the pace of nuclei proliferation are not distinguishable from the WT until the eighth cycle of mitosis takes place. At this stage, the endosperm contains 200 nuclei and, whereas it cellularises in the WT, no cellularisation is observed in the mutant (Fig. 7C,F) where cyst and nodules overgrowth is detected. Later on, at the WT torpedo stage, overgrowth of nodules and a large development of the cyst are dramatic in *msi1/MSI1* seeds (Fig. 6C). However, at this stage of development, endosperm in mutant seeds is smaller than in WT. This is accompanied by a reduced proliferation of endosperm nuclei in comparison with WT (Table 2).

In conclusion, the *msi1-2* mutation causes a severe gametophytic maternal effect on endosperm and embryo development, and a distinct sporophytic recessive embryo lethality. The pace and pattern of cell and nuclei divisions are severely affected in *msi1/msi1* embryo and endosperm, as early as the octant stage in the WT embryo. The gametophytic maternal effect causes the arrest of embryo development and affects several features of endosperm development as other *fis* mutations. But, unlike other mutations (Kiyosue et al., 1999; Vinkenoog et al., 2000), the *msi1* gametophytic maternal phenotype includes a reduction of growth and proliferation of endosperm after the stage when WT endosperm cellularises.

msi1 and *bga* mutations promote autonomous seed development

The mutants *mea*, *fis2* and *fie* are able to initiate endosperm development in the absence of fertilisation. Autonomous endosperm development is accompanied by increase in pistil elongation, which was used as a criterion to identify alleles representative of several *fis* class loci (Fig. 8A-G). We observed very little or no pistil elongation for *dme-4* as reported for *dme-1* (Choi et al., 2002). In contrast, pistil elongation was marked for the other loci, with increasing strength in the following order, *bga*, *mea*, *fis2*, *fie* and *msi1*. Endosperm development is characterised by an increase in ovule size leading to a small developing seed that contains autonomous endosperm (Ohad et al., 1996; Chaudhury et al., 1997). We quantified the penetrance of mutations at each locus by counting the number of autonomous seeds relative to the total number of ovules that are likely to carry the mutation (Table 3, Fig. 8H-N). The penetrance of each mutation is correlated with the degree of pistil elongation. While no autonomous seed development was observed in *dme/DME*, 25-92% of the mutant ovules of other *fis/FIS* plants undergo some degree of seed development in the absence of fertilisation. The allele *msi1-2* has the highest rate of autonomous seed development, with a penetrance of 92%, suggesting that almost every ovule that inherits the *msi1-2* mutation undergoes autonomous seed development. We conclude that, unlike *dme*, which does not promote autonomous seed development, *bga* and *msi1* represent true new members of the *fis* class of mutants. As observed for alterations of endosperm development and penetrance of seed abortion, *bga* has the weakest effects on autonomous seed development while *msi1* causes the strongest defect in this trait.

Table 3. The *fis* class mutants *bga-1* and *msi1-2* undergo autonomous seed development

Line	No. autonomous seeds	No. undeveloped ovules	% seeds/ total ovules (±s.d.)	Penetrance
dme-4/DME	0	532	0	0
mea-6/MEA	70	292	20.6±11.5	41.2
fis2-6/FIS2	86	189	31.7±14.4	63.4
fie-11/FIE	166	265	38.5±11.4	77.0
bga-1/BGA	24	168	12.8±6.4	25.6
msi1-2/MSI1	264	320	46.2±10.4	92.4

Heterozygous mutants (one from each group) were emasculated. Number of seeds (enlarged ovules) and undeveloped ovules was determined 7 days after emasculation. % seeds are the percentage of ovules that undergo autonomous development. Penetrance estimates the percentage of ovules carrying the mutation that undergo autonomous development.

Demethylated pollen restores ectopic GFP expression in *mea*, *fis2*, *dme* and *bga* but not in *fie* and *msi1*

It has been shown that pollination of a WT plant by a demethylated genome reduces the size of the resultant seeds (Adams et al., 2000). When fertilised by pollen from a *METHYLTRANSFERASE1* antisense transgenic line (*MET1* a/s), in which global genome methylation is reduced to 20% of the WT level (Finnegan et al., 1996), *mea*, *fis2* or *fie* ovules develop into seeds whose size and shape are close to WT (Luo et al., 2000; Vinkenoog et al., 2000). This has been interpreted as a rescue of *fis* phenotype by introducing a demethylated paternal genome or by the dominant effect of the *MET1* a/s transgene. We observed the same result with the other gametophytic maternal mutants: *dme*/*DME* × *MET1* a/s siliques contained 52.8% large seeds (n=193), *bga*/*BGA* × *MET1* a/s cross produced 30.4% large seeds (n=269) and *msi1/MSI1* × *MET1* a/s showed 45.5% large seeds (n=213).

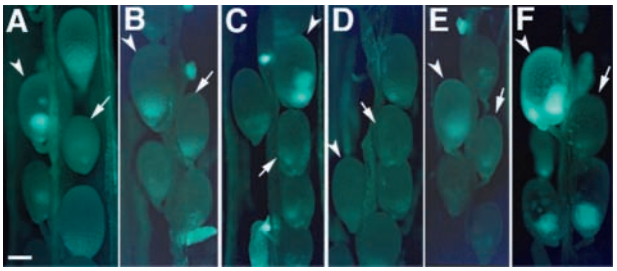

Fig. 9. KS117 GFP marker expression 9 days after pollination of heterozygous gametophytic maternal mutants by a demethylated genome. (A) *mea-6*/*MEA* × *MET1* a/s; (B) *fis2-6*/*FIS2* × *MET1* a/s; (C) *fie-11*/*FIE* × *MET1* a/s; (D) *dme-4*/*DME* × *MET1* a/s; (E) *bga-1*/*BGA* × *MET1* a/s; (F) *msi1-2*/*MSI1* × *MET1* a/s. Two types of seeds are produced when *fis*/*FIS* mutants are fertilised by demethylated *MET1* a/s pollen: the small seeds (arrows) result from WT ovule development, the large seeds (arrowheads) from mutant ovules. GFP expression is low and restricted to the posterior pole in small seeds. In *mea*/*MEA* (A), *fis2*/*FIS2* (B), *dme*/*DME* (D) and *bga*/*BGA* (E) seeds, KS117 GFP expression is properly restricted to the cyst, even when this structure is larger than in WT (A). In contrast, in *fie*/*FIE* (C) and *msi1*/*MSI1* (F) seeds, KS117 GFP is over-expressed and not restricted to the posterior cyst (arrowheads), as when pollinated by WT. Scale bar: 200 μm (all images).

Thus, fertilisation by demethylated pollen seems to rescue the visible phenotypes in the three new mutants *dme*, *bga* and *msi1*, as was described for *mea*, *fis2* and *fie*. In order to investigate whether *MET1* a/s pollination was also able to rescue the GFP expression phenotype, we examined the GFP expression in siliques resulting from pollination of *fis*/*FIS*; KS117/KS117 plants with pollen from homozygous *MET1* a/s plants (Fig. 9). Nine days after pollination, KS117 expression was weak and restricted to the posterior pole in small seeds that had inherited the WT maternal *FIS* allele. In contrast, large seeds presented various KS117 expression patterns, depending on the *fis* locus. In *mea*, *fis2*, *dme* and *bga* seeds (Fig. 9A,B,D,E) KS117 expression was restricted to the posterior cyst, as in WT (n=39, 194, 134 and 154, respectively). In contrast, seeds that maternally inherited the *fie* (18 seeds/56) or *msi1* (34 seeds/71) alleles presented a strong uniform KS117 expression as if they had been pollinated by WT pollen (Fig. 9C,F). These results suggest that the rescue of the gametophytic maternal effect by a demethylated male genome uses alternative pathways depending on the *FIS* gene involved.

Discussion

The endosperm posterior pole development involves oriented nuclear migrations that are under the control of the MEA/FIE PcG complex

The origin of the multiple nuclei present in nodules and in the cyst of the posterior pole endosperm was unclear since no mitosis was ever observed at this pole. Dynamic analysis showed that NCDs migrate towards the cyst and merge together to constitute multinucleate nodules. In turn, these nodules migrate and merge into the cyst that becomes multinucleate. After endosperm cellularisation, the pool of free NCDs becomes limited and remaining NCDs and nodules gradually merge into the cyst. The posterior pole ultimately consists of a large multinucleate cyst that is gradually compressed by the growing embryo after the torpedo stage. The migration of NCDs is oriented towards the posterior pole, indicating that structural features are organised in a polar fashion toward the posterior pole. The nature of these structural elements remains to be identified. Potential candidates are microtubules that have been reported to be organised in an orientation compatible with their use as tracks for migration of NCDs (Brown and Lemmon, 2001). However, the speed of migration of NCDs is at least 50 times slower than the speed recorded for migration of organelles along microtubules (Pollock et al., 1998; Carter et al., 2003). Alternatively, actin filaments may be suitable candidates, although no actin cable was reported at the posterior pole of endosperm in *Coronopus didymus*, a relative of *Arabidopsis* (Nguyen et al., 2002). Nuclear migrations have been inferred during the early endosperm development in Maize (Walbot, 1994) and in *Arabidopsis* (Mansfield and Briarty, 1990) from the analysis of fixed material. Thus, dynamic localisation of nuclei in the syncytial endosperm is a conserved feature but its mechanism remains unknown.

We had reported that *fis* mutations affect the organisation of the posterior pole with overproliferation in nodules that could be located at ectopic position (Sørensen et al., 2001). We show in this study that *fis* mutations impair the migrations of NCDs to the posterior pole. As NCDs do not migrate or migrate at random, they eventually merge at a location distant from the posterior pole and form nodules at ectopic positions. The tight regulation of NCD migration, at least in part, is under the control of the MEA/FIE PcG complex. It can be proposed that the MEA/FIE PcG complex regulates structural features, such as the cytoskeleton, involved in endosperm polarity and NCD migration. According to an alternative hypothesis, the absence of NCD migration in the *fis* mutants could reflect a general delay of endosperm development. However, such a hypothesis should involve a reduction of growth and nuclear proliferation. This is not observed during *fis* endosperm development. We therefore propose that the absence of NCD migration in *fis* mutants reveals impairment of a specific mechanism rather than a global developmental delay.

Maternal control of development of the endosperm posterior pole depends on the conserved MEA/FIE Polycomb Group complex

We identified ten gametophytic maternal mutants showing a *fis* phenotype of the KS117 GFP expression pattern. Of these ten mutants, eight are allelic to *mea*, *fis2*, *fie* or *dme*. Table S1 (http://dev.biologists.org/supplemental/) compiles all the known and new mutant alleles for each of these loci. Genetic mapping identified two other loci, *bga* and *msi1*, at locations distinct from that of other known *fis* mutants. We have identified one allele for each of these two loci.

The definition of the *fis* class of mutants was based on the common ability of *mea*, *fis2* and *fie* mutants to initiate autonomous seed development. Whereas *dme* does not show this trait, the new mutants *bga* and *msi1* demonstrated autonomous endosperm development. We also show that, as described for other *fis* mutants (Kiyosue et al., 1999; Vinkenoog et al., 2000), the development of seeds that maternally inherit *bga* or *msi1* is phenotypically normal until endosperm cellularisation. From this stage, developmental defects, including perturbation of the posterior pole formation

and decrease in seed viability due to embryo arrest, are observed. Ectopic nodules observed in *msi1* and *bga* probably result from the impaired migration of NCDs although we have not performed dynamic observations in these backgrounds. Thus, the two new loci we identified on the basis of their gametophytic maternal control on endosperm development share all the typical characteristics of the *fis* phenotype with the exception of endosperm overproliferation at late stages, and may constitute additional members of the MEA/FIE PcG complex.

Members of the FIS class represent members of a conserved PcG complex

Our finding that *medicis* is mutated in the gene encoding MSI1 supports the recent demonstration of MSI1 as part of the MEA/FIE PcG protein complex (Köhler et al., 2003a). MEA, FIS2 and FIE are homologues of the *Drosophila* PcG proteins E(Z), SU(Z)12 and ESC, respectively that participate in a 600 kDa complex (Tie et al., 2001). This PcG complex has been analysed in detail and contains p55, the homologue of MSI1. This strongly suggests a conservation of the PcG E(Z)/ESC complex between plants and animals.

In this study we describe the new *fis* class mutant *bga*. Penetrance in *bga* mutant is weak, suggesting that either our unique allele *bga-1* is a weak allele, or the BGA protein may form a specific transient complex with the conserved MEA/FIE core complex. In *Drosophila* the histone deacetylase RPD3 has been shown to be part of the 600 kDa E(Z)/ESC complex in embryos (Tie et al., 2001). However, although the *Arabidopsis* genome contains ten members of the RPD3 family (Pandey et al., 2002), none of them is located in the vicinity of the *bga* locus. Alternatively, *bga* might be defective in a regulator of expression or imprinting of the *FIS* genes such as DME (Choi et al., 2002).

Interestingly, besides the embryo arrest provoked by the maternal loss of function of *MSI1*, we observed in *msi1-2* an embryonic phenotype under a sporophytic recessive control. If the seed inherits paternal and maternal *msi1-2* alleles, the embryo pattern is disrupted by cell divisions with a random orientation leading to an early arrest. Consistently abnormally enlarged nucleoli are observed in endosperm suggesting an improper control of nuclear division. *MSI1* is known to be part of *Arabidopsis* Chromatin Assembly Factor-1 (CAF-1), together with FASCIATA1 and FASCIATA2 (Kaya et al., 2001). In vitro assays show that CAF-1 has a replication-dependent nucleosome assembly activity. Furthermore, Ach et al. (Ach et al., 1997) have shown that the tomato homologue of MSI1, LeMSI1, interacts with Retinoblastoma (Rb)-like RBB1 protein from Maize. Hennig et al. (Hennig et al., 2003) also suggest that *Arabidopsis* MSI1 is able to interact with *Arabidopsis* Rb-related RBR protein. As it is known in animals that Rb is involved in G_1 phase progression (reviewed by Weinberg, 1995), it is possible that MSI1 represents a link that has already been suspected in animals between chromatin remodelling by PcG and the control of the cell cycle (Jacobs and van Lohuizen, 2002).

The *fis* alleles were kindly provided by A. Chaudhury and the *MET1* a/s line was generously provided by J. Finnegan. We thank Prof. C. Dumas for hosting our team in his laboratory Reproduction et Développement des Plantes. We thank A. Tissier for seed mutagenesis performed at the Commissariat à l'Energie Atomique, Centre de Cadarache. We thank B. Schindelholz and E. Hafen at The Genetics Company Inc., Schlieren, Switzerland, for their help with DHPLC to identify molecular lesions in the mutants. We thank A. Bendahmane at URGV, Evry, France, for the gift of CelI that contributed to preliminary identification of molecular lesions in the mutants. A.-E.G. is funded by the French Ministry of Research and Education, D.P. was supported by the Roche Research Foundation, work on gametophytic mutants in the Grossniklaus lab is supported by the Kanton of Zürich, and grant 31-64061.00 from the Swiss National Science Foundation. F.B. and P.C. are funded by INRA and J.-E.F. and C.L. are supported by the CNRS. F.B. is part of the EMBO Young Investigator Program. This project was sustained by the program Action Concertée Incitative Jeune and by Génoplante.

References

Ach, R. A., Taranto, P. and Gruissem, W. (1997). A conserved family of WD-40 proteins binds to the retinoblastoma protein in both plants and animals. *Plant Cell* **9**, 1595-1606.

Adams, S., Vinkenoog, R., Spielman, M., Dickinson, H. G. and Scott, R. J. (2000). Parent-of-origin effects on seed development in *Arabidopsis thaliana* require DNA methylation. *Development* **127**, 2493-2502.

Berger, F. and Gaudin, V. (2003). Chromatin dynamics and *Arabidopsis* development. *Chromosome Res.* **11**, 277-304.

Boisnard-Lorig, C., Colon-Carmona, A., Bauch, M., Hodge, S., Doerner, P., Bancharel, E., Dumas, C., Haseloff, J. and Berger, F. (2001). Dynamic analyses of the expression of the HISTONE::YFP fusion protein in *Arabidopsis* show that syncytial endosperm is divided in mitotic domains. *Plant Cell* **13**, 495-509.

Brown, R. C., Lemmon, B. E., Nguyen, H. and Olsen, O.-A. (1999). Development of endosperm in *Arabidopsis thaliana*. *Sex Plant Reprod.* **12**, 32-42.

Brown, R. C. and Lemmon, B. E. (2001). The cytoskeleton and spatial control of cytokinesis in the plant life cycle. *Protoplasma* **215**, 35-49.

Carter, G. C., Rodger, G., Murphy, B. J., Law, M., Krauss, O., Hollinshead, M. and Smith, G. L. (2003). Vaccinia virus cores are transported on microtubules. *J. Gen. Virol.* **84**, 2443-2458.

Castle, L. A., Errampalli, D., Atherton, T. L., Franzmann, L. H., Yoon, E. S. and Meinke, D. W. (1993). Genetic and molecular characterization of embryonic mutants identified following seed transformation in *Arabidopsis*. *Mol. Gen. Genet.* **241**, 504-514.

Chaudhury, A. M., Ming, L., Miller, C., Craig, S., Dennis, E. S. and Peacock, W. J. (1997). Fertilization-independent seed development in *Arabidopsis thaliana*. *Proc. Natl. Acad. Sci. USA* **94**, 4223-4228.

Choi, Y., Gehring, M., Johnson, L., Hannon, M., Harada, J. J., Goldberg, R. B., Jacobsen, S. E. and Fischer, R. L. (2002). DEMETER, a DNA Glycosylase Domain Protein, Is Required for Endosperm Gene Imprinting and Seed Viability in *Arabidopsis*. *Cell* **110**, 33-42.

Finnegan, E. J., Peacock, W. J. and Dennis, E. S. (1996). Reduced DNA methylation in *Arabidopsis thaliana* results in abnormal plant development. *Proc. Natl. Acad. Sci. USA* **93**, 8449-8454.

Floyd, S. K. and Friedman, W. E. (2000). Evolution of endosperm developmental patterns among basal flowering plants. *Int. J. Plant Sci.* **161 Suppl. S**, S57-S81.

Garcia, D., Saingery, V., Chambrier, P., Mayer, U., Jürgens, G. and Berger, F. (2003). *Arabidopsis* haiku mutants reveal new controls of seed size by endosperm. *Plant Physiol.* **131**, 1661-1670.

Grossniklaus, U., Vielle-Calzada, J. P., Hoeppner, M. A. and Gagliano, W. B. (1998). Maternal control of embryogenesis by *MEDEA*, a polycomb group gene in *Arabidopsis*. *Science* **280**, 446-450.

Haseloff, J. (1999). GFP variants for multispectral imaging of living cells. *Methods Cell Biol.* **58**, 139-151.

Hebsgaard, S. M., Korning, P. G., Tolstrup, N., Engelbrecht, J., Rouze, P. and Brunak, S. (1996). Splice site prediction in *Arabidopsis thaliana* pre-mRNA by combining local and global sequence information. *Nucleic Acids Res.* **24**, 3439-3452.

Hennig, L., Taranto, P., Walser, M., Schonrock, N. and Gruissem, W. (2003). *Arabidopsis* MSI1 is required for epigenetic maintenance of reproductive development. *Development* **130**, 2555-2565.

Jacobs, J. J. L. and van Lohuizen, M. (2002). Polycomb repression: from

cellular memory to cellular proliferation and cancer. *Biochim. Biophys. Acta* **1602**, 151-161.

Jander, G., Norris, S. R., Rounsley, S. D., Bush, D. F., Levin, I. M. and Last, R. L. (2002). *Arabidopsis* map-based cloning in the post-genome era. *Plant Physiol.* **129**, 440-450.

Jürgens, G., Mayer, U., Torres-Ruiz, R. A., Berleth, T. and Miséra, S. (1991). Genetic analysis of pattern formation in the *Arabidopsis* embryo. *Development* **Suppl. 1**, 27-38.

Kaya, H., Shibahara, K.-I., Taoka, K.-I., Iwabuchi, M., Stillman, B., Araki, T. (2001). *FASCIATA* genes for Chromatin Assembly Factor-1 in *Arabidopsis* maintain the cellular organization of apical meristems. *Cell* **104**, 131-142.

Kiyosue, T., Ohad, N., Yadegari, R., Hannon, M., Dinneny, J., Wells, D., Katz, A., Margossian, L., Harada, J. J., Goldberg, R. B. and Fischer, R. L. (1999). Control of fertilization-independent endosperm development by the MEDEA polycomb gene in *Arabidopsis*. *Proc. Natl. Acad. Sci. USA* **96**, 4186-4191.

Köhler, C., Hennig, L., Bouveret, R., Gheyselinck, J., Grossniklaus, U. and Gruissem, W. (2003a). *Arabidopsis* MSI1 is a component of the MEA/FIE Polycomb group complex and required for seed development. *EMBO J.* **22**, 4804-4814.

Köhler, C., Hennig, L., Spillane, C., Pien, S., Gruissem, W. and Grossniklaus, U. (2003b). The Polycomb-group protein MEDEA regulates seed development by controlling expression of the MADS-box gene PHERES1. *Genes Dev.* **17**, 1540-1553.

Luo, M., Bilodeau, P., Koltunow, A., Dennis, E. S., Peacock, W. J. and Chaudhury, A. M. (1999). Genes controlling fertilization-independent seed development in *Arabidopsis thaliana*. *Proc. Natl. Acad. Sci. USA* **96**, 296-301.

Luo, M., Bilodeau, P., Dennis, E. S., Peacock, W. J. and Chaudhury, A. (2000). Expression and parent-of-origin effects for *FIS2*, *MEA*, and *FIE* in the endosperm and embryo of developing *Arabidopsis* seeds. *Proc. Natl. Acad. Sci. USA* **97**, 10637-10642.

Mansfield, S. G. and Briarty, L. G. (1990). Development of the free-nuclear endosperm in *Arabidopsis thaliana*. *Arabidopsis Inf. Serv.* **27**, 53-64.

Nguyen, H., Brown, R. C. and Lemmon, B. E. (2002). Cytoskeletal organization of the micropylar endosperm in *Coronopus didymus* L. (Brassicaceae). *Protoplasma* **219**, 210-220.

Ohad, N., Margossian, L., Hsu, Y. C., Williams, C., Repetti, P. and Fischer, R. L. (1996). A mutation that allows endosperm development without fertilization. *Proc. Natl. Acad. Sci. USA* **93**, 5319-5324.

Ohad, N., Yadegari, R., Margossian, L., Hannon, M., Michaeli, D., Harada, J. J., Goldberg, R. B. and Fischer, R. L. (1999). Mutations in FIE, a WD polycomb group gene, allow endosperm development without fertilization. *Plant Cell* **11**, 407-416.

Pandey, R., Muller, A., Napoli, C. A., Selinger, D. A., Pikaard, C. S., Richards, E. J., Bender, J., Mount, D. W. and Jorgensen, R. A. (2002). Analysis of histone acetyltransferase and histone deacetylase families of *Arabidopsis thaliana* suggests functional diversification of chromatin modification among multicellular eukaryotes. *Nucleic Acids Res.* **30**, 5036-5055.

Peacock, J., Ming, L., Craig, S., Dennis, E. and Chaudhury, A. (1995). A mutagenesis programme for apomixis genes in *Arabidopsis*. In *Induced Mutations and Molecular Techniques for Crop Improvement*, pp. 117-125. Vienna, Austria: IAEA.

Pollock, N., Koonce, M. P., de-Hostos, E. L. and Vale, R. D. (1998). In vitro microtubule-based organelle transport in wild-type Dictyostelium and cells overexpressing a truncated dynein heavy chain. *Cell Motil. Cytoskeleton* **40**, 304-314.

Raghavan, V. (2003). Some reflections on double fertilization, from its discovery to the present. *New Phytol.* **159**, 565-583.

Reyes, J. C. and Grossniklaus, U. (2003). Diverse functions of Polycomb group proteins during plant development. *Semin. Cell Dev. Biol.* **14**, 77-84.

Scott, R. J., Spielman, M., Bailey, J. and Dickinson, H. G. (1998). Parent-of-origin effects on seed development in *Arabidopsis thaliana*. *Development* **125**, 3329-3341.

Sørensen, M. B., Chaudhury, A. M., Robert, H., Bancharel, E. and Berger, F. (2001). Polycomb group genes control pattern formation in plant seed. *Curr. Biol.* **11**, 277-281.

Sørensen, M. B., Mayer, U., Lukowitz, W., Robert, H., Chambrier, P., Jürgens, G., Somerville, C., Lepiniec, L. and Berger, F. (2002). Cellularisation in the endosperm of *Arabidopsis thaliana* is coupled to mitosis and shares multiple components with cytokinesis. *Development* **129**, 5567-5576.

Spillane, C., MacDougall, C., Stock, C., Köhler, C., Vielle-Calzada, J. P., Nunes, S. M., Grossniklaus, U. and Goodrich, J. (2000). Interaction of the *Arabidopsis* polycomb group proteins FIE and MEA mediates their common phenotypes. *Curr. Biol.* **10**, 1535-1538.

Tie, F., Furuyama, T., Prasad-Sinha, J., Jane, E. and Harte, P. J. (2001). The Drosophila Polycomb Group proteins ESC and E(Z) are present in a complex containing the histone-binding protein p55 and the histone deacetylase RPD3. *Development* **128**, 275-286.

Vinkenoog, R., Spielman, M., Adams, S., Fischer, R. L., Dickinson, H. G. and Scott, R. J. (2000). Hypomethylation promotes autonomous endosperm development and rescues postfertilization lethality in fie mutants. *Plant Cell* **12**, 2271-2282.

Walbot, V. (1994). Overview of key steps in aleurone development. In *The Maize Handbook*, pp. 78-80. New York: Springer-Verlag.

Weinberg, R. A. (1995). The retinoblastoma protein and cell cycle. *Cell* **81**, 323-330.

Yadegari, R., Kinoshita, T., Lotan, O., Cohen, G., Katz, A., Choi, Y., Nakashima, K., Harada, J. J., Goldberg, R. B., Fischer, R. L. and Ohad, N. (2000). Mutations in the *FIE* and *MEA* genes that encode interacting polycomb proteins cause parent-of-origin effects on seed development by distinct mechanisms. *Plant Cell* **12**, 2367-2381.

Table S1. Summary of published mutant alleles of *FIS* genes

Allele	Mutagenesis	Reference
fis1/mea	EMS	(Peacock et al., 1995; Chaudhury et al., 1997; Luo et al., 1999)
mea-1, mea-2	Ds insertion	(Grossniklaus et al., 1998)
mea-3, mea-4	EMS	(Castle et al., 1993; Kiyosue et al., 1999)
mea-5, mea-6, mea-7	Gamma ray	This study
fis2-1, fis2-3, fis2-4	EMS	(Peacock et al., 1995; Luo et al., 1999)
fis2-2	Ds insertion	(Luo et al., 1999)
fis2-5		(Köhler et al., 2003b)
fis2-6, fis2-7	Gamma ray	This study
fis3/fie	EMS	(Peacock et al., 1995; Chaudhury et al., 1997)
fie-1, fie-2, fie-3, fie-4, fie-5, fie-6, fie-9	EMS	(Ohad et al., 1999)
fie-7, fie-8		(Ohad et al., 1999)
fie-10, fie-11	Gamma ray	This study
dme-1, dme-2, dme-3	T-DNA insertion	(Choi et al., 2002)
dme-4	Gamma ray	This study
msi1-1	T-DNA insertion	(Köhler et al., 2003a)
msi1-2	Gamma ray	This study
bga-1	Gamma ray	This study